

Published in final edited form as:

*Oral Oncol.* 2013 October ; 49(10): 991–997. doi:10.1016/j.oraloncology.2013.07.006.

## A novel extracellular drug conjugate significantly inhibits head and neck squamous cell carcinoma

Larissa Sweeny<sup>a</sup>, Yolanda E. Hartman<sup>a</sup>, Kurt R. Zinn<sup>b</sup>, James R. Prudent<sup>c</sup>, David J. Marshall<sup>c</sup>, Mohammed S. Shekhani<sup>c</sup>, and Eben L. Rosenthal<sup>a,\*</sup>

<sup>a</sup>University of Alabama at Birmingham, Department of Surgery, Division of Otolaryngology – Head and Neck Surgery, 1670 University Boulevard, Volker Hall G082, Birmingham, AL 35233, USA

<sup>b</sup>University of Alabama at Birmingham, Department of Radiology, 1670 University Boulevard, Volker Hall G082, Birmingham, AL 35233, USA

<sup>c</sup>Centrose LLC, 802 Deming Way, Madison, WI 53717-1917, USA

### Abstract

**Objectives**—Despite advances in treatment modalities, head and neck squamous cell carcinoma (HNSCC) remains a challenge to treat with poor survival and high morbidity, necessitating a therapy with greater efficacy. EDC22 is an extracellular drug conjugate of the monoclonal antibody targeting CD147 (glycoprotein highly expressed on HNSCC cells) linked with a small drug molecule inhibitor of Na, K-ATPase. In this study, EDC22's potential as a treatment modality for HNSCC was performed.

**Materials and methods**—HNSCC cell lines (FADU, OSC-19, Cal27, SCC-1) were cultured in vitro and proliferation and cell viability were assessed following treatment with a range of concentrations of EDC22 (0.25–5.00 µg/mL). Mice bearing HNSCC xenografts (OSC-19, SCC-1) were treated with either EDC22 (3–10 mg/kg), anti-CD147 monoclonal antibody, cisplatin (1 mg/kg) or radiation therapy (2 Gy/week) monotherapy or in combination.

**Results**—In vitro, treatment with minimal concentration of EDC22 (0.25 µg/mL) significantly decreased cellular proliferation and cell viability ( $p < 0.0001$ ). In vivo, systemic treatment with EDC22 significantly decreased primary tumor growth rate in both an orthotopic mouse model (OSC-19) and a flank tumor mouse model (SCC-1) ( $p < 0.05$ ). In addition, EDC22 therapy resulted in a greater reduction in tumor growth in vivo compared to radiation monotherapy ( $p < 0.05$ ) and a similar reduction in tumor growth compared to cisplatin monotherapy. Combination therapy provided no significant further reduction in tumor growth relative to EDC22 monotherapy.

**Conclusion**—EDC22 is a potent inhibitor of HNSCC cell proliferation in vitro and in vivo, warranting further investigations of its clinical potential in the treatment of HNSCC.

### Keywords

Aerodigestive squamous cell carcinoma; Head and neck; Extracellular drug conjugate; CD147

---

© 2013 Elsevier Ltd. All rights reserved.

\*Corresponding author. Tel.: +1 (205) 934 9766; fax: +1 (205) 934 3993. oto@uab.edu (E.L. Rosenthal).

#### Conflict of interest statement

Centrose, LLC, the company that produced EDC22, employs the following authors: James R. Prudent, David J. Marshall, and Mohammed S. Shekhani. The remaining authors have nothing to disclose.

## Introduction

Several advances in treatment modalities for head and neck squamous cell carcinoma (HNSCC) have been made over the past several decades. These include targeted radiation therapy (Gamma Knife and Cyber Knife) as well as various chemotherapeutics (platinum therapies, targeted monoclonal antibodies). Despite these advances, prognosis and survival has only minimally improved in this patient population [1–9]. Survival of head and neck cancer patients has slightly improved following the use local therapies, such as surgery or radiotherapy, in large part due to locoregional and distant metastatic failure [10]. While, systemic monotherapy using platinum based compounds have limited response rates except when combined with radiotherapy [11–14]. Whereas, targeted systemic therapy with monoclonal antibodies lacks the potency necessary to completely halt tumorigenesis resulting in varied response rates and limited improvement in survival rates [15]. Delivery of highly toxic, but non-selective, small molecule inhibitors are associated with harmful side effects and result in significant injury to normal tissues. Antibody–drug conjugates provide the potential to improve the therapeutic index of these toxic agents by conjugating them with targeted therapies, such as monoclonal antibodies, capable of directing the drug conjugate to the tumor cells and minimalizing exposure to normal cells. Several antibody drug conjugate therapies are currently in clinical trials or have recently been FDA approved. These include, but are not limited to, therapies for myeloid leukemia (target: CD33), Hodgkin’s lymphoma (target: CD30), breast cancer (target: HER2/neu), small cell lung cancer (target: CD56), melanoma (target: GPNMB), B-cell lymphoma (target: CD19), and ovarian (target: EphA2, CA6) [16]. This investigation sought to determine the efficacy of an antibody–drug conjugate linking a small molecule inhibitor of Na,K-ATPase to a monoclonal antibody targeting the transmembrane protein CD147.

Na,K-ATPase is an enzymatic component of Na,K-ATP channels found on cell membranes. The Na,K-ATP channel is essential to maintaining cell volume and regulating the electrical potential of a cell. When the Na,K-ATPase is inhibited, sodium accumulates in the cell increasing intracellular osmosis until the cell bursts [17,18]. Unconjugated small molecule inhibitors capable of inhibiting Na,K-ATPase are non-specific resulting in high toxicity to normal cells. However, conjugation with a monoclonal antibody targeting proteins overexpressed by oncologic cells, would minimize the exposure of normal cells to the Na,K-ATPase inhibitor. This would reduce toxicity, increase the therapeutic index and improve efficacy.

Monoclonal antibodies are capable of providing selective therapy by selecting for extracellular or transmembrane proteins that are highly expressed on tumor cells with limited expression on normal cells. This allows the monoclonal antibody to accumulate on tumor cells specifically, reducing side effects and allowing for higher dosing. Unfortunately, these therapies have had varied clinical responses, often unrelated to the protein expression pattern of the tumor cells. This is thought to be in part the product of the resilient and adaptive characteristic of tumor cells. With a multitude of intra- and extracellular signaling pathways, oncologic cells are able to survive, and sometimes flourish, despite the blockade of one of the pathways with a monoclonal antibody. As a result, there is a need for novel and more potent therapeutics.

CD147 is transmembrane glycoprotein highly expressed on head and neck cancer cells with very limited expression in normal tissues [19–22]. In fact, in oral epithelium expression of CD147 gradually increases with de-differentiation of the basal epithelial layer [8,23,24] Expression of CD147 has been shown to provide a survival advantage to cells by promotion of cell proliferation and facilitating cell migration and invasion [25–29]. Adjacent to CD147 on the cell membrane resides the Na,K-ATPase as part of a larger complex [30]. Due to the

selective expression of CD147 on tumor cells and the proximity to Na,K-ATP channels, we hypothesized that delivery of an extracellular drug conjugate (EDC) linking a Na,K-ATPase inhibitor to an anti-CD147 monoclonal antibody may result in a highly toxic chemotherapeutic agent. This study evaluated the feasibility and potency of this EDC (EDC22) in the treatment of HNSCC cells in vitro and in vivo.

## Materials and methods

### Cell lines and tissue culture

Several human HNSCC tumor cell lines were investigated: SCC-1 (University of Michigan), OSC-19 (University of Texas, MD Anderson), FADU and Cal27 (American Type Culture Collection, Rockville, MD). The cells were maintained in DMEM and supplemented with 10% fetal bovine serum and 1% penicillin–streptomycin solution. Cells were incubated at 37 °C in a humidified atmosphere containing 5% CO<sub>2</sub>.

### Reagents

The anti-CD147 monoclonal antibody (clone 1A6) was constructed at the University of Alabama at Birmingham (Tong, Z). The small drug molecule targeting Na,K-ATPase and the extracellular drug conjugate (EDC22) was produced by Centrose LLC (Madison, Wisconsin). Briefly, using the Centrose Carbo Connect<sup>®</sup> platform (capable of creating and screening sugar enhanced libraries from known drugs) and scillarenin (drug precursor), a set of differentially glycosylated bufadienolides was discovered. Differential glycosylation has been found to increase anticancer activity [31]. These glycosylated bufadienolides contained a primary amine used for standard conjugation chemistries resulting in the prototype EDC. The required intramolecular distance between the binding epitope and the primary amine (bound to Na<sup>+</sup>,K<sup>+</sup>-ATPase in the context of the functional complex), was determined using a structural model derived from a prototypical antibody (mouse IgG antibody) [32] and an existing structure for a Na<sup>+</sup>,K<sup>+</sup>-ATPase complex [33]. An estimation of the distance between the antibody hinge region disulfides and the drug binding pocket was then calculated (~95 Å). A water soluble polyethylene oxide chain linker (24 repeating PEG subunits) was chosen. A non-cleavable heterobifunctional linker (N-hydroxysuccinimide ester on proximal end and an orthogonal maleimide on distal terminus) [34–39] was used for the conjugation of the bufadienolide amino-glycosides. A competitive ELISA and drug specific ELISA (antibody specific for the core structure of small molecules) was used to assess epitope recognition by the conjugates. Data suggest the conjugates maintain strong target recognition as well as a potent small molecule inhibitor. Treatment efficacy of the conjugate (EDC22) was compared to cisplatin (Sigma–Aldrich, St. Louis, MO) and radiation therapy (X-RAD 320, RPS Services, Surrey, KT).

### Western blot analysis

Cells were grown to 70–80% confluence, washed twice with cold PBS, and lysed in lysis buffer [50 mM Tris–HCl (pH 7.5), 150 mM NaCl, 1% (v/v) NP40, 0.5% (w/v) sodium deoxycholate, 1 mM EDTA, 0.1% SDS], and a protease inhibitor cocktail tablet (Roche Applied Science, Indianapolis, IN) was added. The cleared lysates were collected by centrifugation at 12000 g for 20 min at 40 °C. The protein concentrations were measured by BCA protein assay (Thermo Scientific, Rockford, IL). Lysates with 10 mg of total protein were resolved by SDS PAGE and transferred to PVDF membranes. The membranes were incubated with the primary antibody (CD147, sc-21746, Santa Cruz Biotechnology, Dallas, TX). After washing and incubating with horseradish peroxidase conjugated secondary antibodies, the membranes were washed again and detected by the Amersham ECL Western blotting detection system (GE healthcare, Buckinghamshire, UK). The membranes were re-probed with horseradish peroxidase-conjugated mouse monoclonal antihuman beta-actin.

### In vitro proliferation assays

To determine the effects of EDC22 on cell proliferation in vitro, HNSCC cells (FADU, SCC-1, OSC-19 and Cal27) were seeded ( $5 \times 10^4$  cells/well) in 48 well tissue culture treated plates (Falcon, Becton Dickinson Labware, Franklin Lakes, NJ), treated in triplicate with EDC22 at increasing concentrations (0, 0.25, 0.50, 1.00, 2.50, 5.00  $\mu\text{g}/\text{mL}$ ; day 0) and incubated for 48 and 72 h. In addition, HNSCC cells were also treated with anti-CD147 mAb (200  $\mu\text{g}/\text{mL}$ ; day 0) for 48 h [40]. On day 2 or day 3 cells were trypsinized and counted with a flow cytometer (Accuri, C6, Ann Arbor, MI).

### In vitro cell viability

The ATPlite luminescence assay (PerkinElmer, Waltham, MA) was used to determine the effects of EDC22 on cell viability in vitro. HNSCC cells (FADU, SCC-1, OSC-19 and Cal27) were seeded ( $1 \times 10^4$  cells/well) in a 96 well tissue culture treated plate (Falcon, Becton Dickinson Labware, Franklin Lakes, NJ), treated in triplicate with EDC22 at increasing concentrations (0, 0.25, 0.50, 1.00, 2.50, 5.00  $\mu\text{g}/\text{mL}$ ; day 0) and incubated for 48 h. On day 2 the assay was performed according to the manufacturer's instructions and read on a Versa Max plate reader (Molecular Devices, Sunnyvale, CA) with Soft Max Pro 5 software (Molecular Devices, Sunnyvale, CA).

### HNSCC xenograft mouse model

Athymic female nude mice aged 6–8 weeks (Charles River Laboratories and National Cancer Institute – Frederick) were obtained and housed in accordance with the Institutional Animal Care and Use Committee (IACUC) guidelines at our institution.

To assess the effect of EDC22 on HNSCC tumor growth in vivo, an orthotopic tongue tumor model was established by injecting OSC-19 cells ( $2.5 \times 10^5$ ) suspended in 30  $\mu\text{L}$  serum-free DMEM into the proximal tongue. For the initial in vivo evaluation of EDC22, cohorts were divided into control, anti-CD147 monoclonal antibody 1A6 (30 mg/kg/wk), EDC22 (3 mg/kg/wk), or EDC22 (10 mg/kg/wk) ( $n = 5$  per group). The optimal dosing of EDC22 was determined to be 3 mg/kg twice a week (see Section Results).

To compare EDC22 therapy to cisplatin or radiation therapy in vivo, a flank tumor model was used. The flank tumor model was used for these experiments due to its improved tolerance by the animals, allowing for longer treatment duration and follow up. SCC-1 cells ( $2.0 \times 10^6$ ) were suspended in 200  $\mu\text{L}$  of serum-free DMEM and injected subcutaneously into the flank of female athymic nude mice ( $n = 5/\text{group}$ ). Treatment response to EDC22 (3 mg/kg biweekly) in vivo was then compared to cisplatin (1 mg/kg/wk) [41,42] or radiation therapy (2 Gy/wk; X-RAD 320, RPS Services, Surrey, KT).

For the treatment cohorts, treatments were administered systemically (tail vein, t.v.) and treatment was initiated once the average volume of the orthotopic tumors was 100–120  $\text{mm}^3$  or the flank tumors had a surface area (length x width) of 16  $\text{mm}^2$ . Orthotopic tumors were measured triweekly (length, width and depth) and flank tumors were measured biweekly (length and width) using calipers to approximate.

### Statistical analyses

Data analyses of in vitro cell growth and in vivo xenografts growth were done using Graph Pad Prism software (Graph Pad Software, Inc., La Jolla, CA). Quantitative data was expressed as a mean  $\pm$  standard deviation (SD). Equation for volume of an ellipsoid [volume =  $(4/3)(3.14)(\text{length})(\text{width})(\text{depth})$ ] was used to calculate in vivo orthotopic tongue tumor volume.  $p < 0.05$  was considered significant in unpaired  $t$ -test analysis used to determine

differences between groups. Western blot band intensities were quantified using ImageJ (<http://rsb.info.nih.gov/ij/>) and normalized to beta-actin.

## Results

### CD147 expression of the cell lines

Using western blot analysis, the relative CD147 expression levels of the HNSCC cells were normalized to beta-actin and their densitometries were compared. Cal27 had the lowest expression of CD147 on densitometry (0.44), followed by OSC-19 (0.70), then FADU (1.10) and SCC-1 (1.31). Stated differently, relative to Cal27: OSC-19 had 1.6 times greater expression, FADU had 2.48 greater expression, and SCC-1 had 2.96 times greater expression of CD147 (data not shown).

### EDC22 profoundly inhibits HNSCC cell proliferation in vitro

Treatment of HNSCC cells with EDC22 in vitro significantly reduced proliferation (Fig. 1). Following only 48 h of treatment, even at the lowest concentration of EDC22 (0.25 µg/mL), cell proliferation was significantly reduced for each HNSCC cell lines ( $p < 0.0001$ ). Relative to control: FADU proliferation was 17.0%, OSC-19 proliferation was 45.5%, Cal27 proliferation was 31.0% and SCC-1 proliferation was 9.6%. For comparison, HNSCC cell lines were also treated with high dose anti-CD147 monoclonal antibody (200 µg/mL) [40] with an observed reduction in proliferation relative to control of 37.1% (FaDu), 71.7% (OSC-19), 77.9% (Cal27), and 71.0% (SCC-1). Proliferation of cells treated with anti-CD147 monoclonal antibody (200 µg/mL) alone was significantly higher for FADU ( $p < 0.0001$ ), OSC-19 ( $p < 0.0001$ ), and Cal27 ( $p < 0.0001$ ) than when treated with any concentration of EDC22.

Increased duration of treatment resulted in significantly higher cytotoxicity. Following 72 h of treatment, there was an even greater reduction in proliferation at each concentration of EDC22 and for all cell lines. Relative to control, proliferation following treatment with EDC22 (0.25 µg/mL) were as follows: 9.5% for FADU cells, 9.1% for OSC-19 cells, 45.9% for Cal27 cells and 9.0% for SCC-1 cells.

### EDC22 profoundly reduces HNSCC cell viability in vitro

To determine the effect of EDC22 on cell viability, we assessed ATP production in a panel of HNSCC cells treated with EDC22 (0–5.0 µg/mL) for 48 h. ATP production of the cells was then measured and found to be significantly reduced by even the lowest dose of EDC22 (0.25 µg/mL) for each HNSCC cell line ( $p < 0.0001$ ) (Fig. 2). Relative to control, ATP production following treatment with EDC22 (0.25 µg/mL) were as follows: 2.5% in FADU cells; 15.1% in OSC-19 cells; 38.7% in Cal27 cells; and 12.1% in SCC-1 cells.

### EDC22 reduced HNSCC growth in an orthotopic nude mouse model

The in vivo antitumor efficacy of EDC22 was evaluated in HNSCC orthotopic xenografts. Treatment cohorts were dosed with anti-CD147 antibody (30 mg/kg/wk), EDC22 (3 mg/kg/wk), or EDC22 (10 mg/kg/wk) systemically for 18 days (Fig. 3). Relative to control and anti-CD147 treatment cohorts, both EDC22 treatment cohorts demonstrated significantly smaller tumor volumes on day 8 and day 10 relative to controls ( $p < 0.01$ ). Interestingly, there was a reduction in tumor volume observed on day 4 and day 6 following the first treatment dose in both EDC22 cohorts. However, small rebound increase in tumor growth was observed on day 8, which again was followed by decreased in tumor volume following the second dose of EDC22. This was observed in both EDC22 treated cohorts. Therefore, it was hypothesized EDC22 was being metabolized by day 6, allowing the tumor cells to



proliferate. For future in vivo experiments, the dosing was increased to twice a week. For both EDC cohorts, a reduction in tumor growth was observed for the duration of the study. Additional reduction in tumor growth was not observed at the higher dosage of EDC22 (10 mg/kg), therefore the lower EDC22 dose (3 mg/kg) were used for subsequent experiments.

### **In vivo treatment with EDC22 is comparable to cisplatin**

In vivo, SCC-1 flank xenografts were divided into four cohorts: control, EDC22 (3 mg/kg/biweekly), cisplatin (1 mg/kg/wk) [41,42], and combination EDC22 and cisplatin. Tumor growth was reported as the fraction change relative to tumor size at the start of treatment (Fig. 4). Relative to control, xenografts treated with EDC22 had significant reduction in tumor growth on days 8 ( $0.80 \pm 0.11$ ;  $p = 0.007$ ), 16 ( $0.82 \pm 0.53$ ;  $p = 0.04$ ), 26 ( $0.77 \pm 0.74$ ;  $p = 0.04$ ), and 30 ( $0.63 \pm 0.57$ ;  $p = 0.046$ ). Similarly, xenografts treated with the combination therapy had a reduction in tumor growth on days 8 ( $0.58 \pm 0.09$ ;  $p = 0.0008$ ), 16 ( $0.54 \pm 0.19$ ;  $p = 0.01$ ), 26 ( $0.12 \pm 0.12$ ;  $p = 0.02$ ), and 30 ( $0.16 \pm 0.16$ ;  $p = 0.015$ ) relative to control. However, there was no significant difference between the tumor growth in the EDC22 and combination therapy cohorts. There was a significant difference between cisplatin monotherapy ( $1.21 \pm 0.23$ ) and combination treatment on day 8 ( $p = 0.009$ ) and relative to control on day 16 ( $0.78 \pm 0.28$ ;  $p = 0.04$ ). Suggesting, combination therapy provided greater reduction in tumor growth than cisplatin monotherapy alone. During the duration of treatment, the weight of the each mouse remained stable or increased (data not shown). Examination of the mice and observation of behavior and feeding did not find evidence of any side effects secondary to the treatments.

### **Tumor growth in vivo was significantly reduced by EDC22 treatment relative to radiation therapy**

SCC-1 flank xenografts were divided into four cohorts: EDC22 (3 mg/kg/biweekly), radiation therapy (2 Gy/wk), and combination EDC22 and radiation therapy. Tumor growth was reported as the fraction change relative to tumor size at the start of treatment (Fig. 5). Xenografts treated with EDC22 had significant reduction in tumor growth on days 7 ( $0.80 \pm 0.11$ ;  $p = 0.004$ ) 10 ( $1.0 \pm 0.14$ ;  $p = 0.008$ ), 14 ( $0.79 \pm 0.10$ ;  $p = 0.03$ ), 17 ( $0.80 \pm 0.28$ ;  $p = 0.038$ ), 32 ( $0.36 \pm 0.29$ ;  $p = 0.006$ ) and day 40 ( $0.36 \pm 0.34$ ;  $p = 0.001$ ) relative control. Similarly, xenografts treated with the combination therapy had a reduction in tumor growth on days 7 ( $0.99 \pm 0.06$ ;  $p = 0.003$ ), 10 ( $0.83 \pm 0.08$ ;  $p = 0.0009$ ), 14 ( $1.02 \pm 0.13$ ;  $p = 0.0498$ ), 17 ( $0.61 \pm 0.11$ ;  $p = 0.047$ ), 32 ( $1.3 \pm 0.14$ ;  $p = 0.018$ ) and day 40 ( $1.5 \pm 0.22$ ;  $p = 0.005$ ). There was also a significant difference between radiation therapy alone on day 7 ( $1.1 \pm 0.14$ ;  $p = 0.007$ ) and day 40 ( $4.5 \pm 1.2$ ;  $p = 0.038$ ) relative to control. However, when both monotherapy cohorts were compared, a greater reduction in tumor growth was found following treatment with EDC22 monotherapy than radiation therapy alone (day 21–day 40;  $p < 0.05$ ). In addition, combination therapy resulted in greater reduction in tumor growth compared to radiation monotherapy (day 21–day40;  $p < 0.05$ ). However, there was no significant difference between the tumor growth in the EDC22 and combination therapy cohorts. During the duration of treatment, the weight of the each mouse remained stable or increased (data not shown). Examination of the mice and observation of behavior and feeding did not find evidence of any side effects secondary to the treatments.

## **Discussion**

Tumor cells have demonstrated significant adaptability and resistance to current treatment modalities. It is evident that more potent therapeutics are required to adequately eradicate malignant cells. Unfortunately, the current highly toxic therapies lack selectivity and subsequently have a narrow therapeutic index. While less toxic targeted therapeutics lack the potency necessary to prevent proliferation of every malignant cell proliferation allowing for

resistance to develop and adaptation by the tumor cells. Combining the potency of a more toxic agent with the specificity of a targeting agent may allow for improved therapeutic efficacy. Extracellular drug conjugates (EDC) link a safe, selective targeting monoclonal antibody with a potent small drug molecule. In this preclinical study the feasibility and efficacy of EDC22, an extracellular drug conjugate linking a potent small molecule inhibitor targeting the external kinase regulator Na,K-ATPase with a specific monoclonal antibody targeting CD147, was investigated.

EDC22 was found to have significant anti-proliferative effects on HNSCC in vitro. Even when treated with extremely low doses of EDC22 (0.25 µg/mL), there was a profound reduction in HNSCC cell proliferation relative to untreated controls. Similarly, there was a significant reduction in HNSCC cell viability in vitro following treatment with even the lowest dose of EDC22. Given these findings, future in vitro experiments would benefit from treatment with a 10 to 100-fold lower concentration range. When the duration from initial treatment dose was extended from 48 h to 72 h, it was expected cell proliferation may stabilize or even increase as the cells adapted to treatment conditions. However, an even greater reduction in cell proliferation was observed.

The effects of EDC22 treatment on HNSCC cells were also assessed in several in vivo experiments. Interestingly, it was found the lower dose of EDC22 (3 mg/kg) resulted in similar reductions in tumor growth compared to the higher dose (10 mg/kg). This suggests lower dosage of the conjugate can be given, producing the same anti-carcinogenic effects while minimizing side effects. Although there were no toxic side effects observed in the xenografts, further experiments investigating the toxicity of EDC22 on normal human cell types expressing CD147 are necessary. The optimal dosage schedule was found to be bi-weekly. When treatments were administered once a week, a slight rebound effect was observed prior to the next dose. We hypothesize this is the result of monoclonal antibody circulation times as well as the challenges of delivering these macromolecules to the core of solid tumors [16]. Increased frequency of dosing may allow for additional cells to be exposed to EDC22 as surface cells undergo apoptosis exposing the cells beneath.

In vivo treatment with EDC22 was compared to monotherapy with a platinum based chemotherapeutic, cisplatin, and in combination. Although these drugs have very different mechanisms of action, this study did not find any additional benefit to treatment with combination therapy compared to EDC22 monotherapy [41,42]. However, a comparison of cisplatin monotherapy to combination therapy found a greater reduction in tumor growth following combination therapy ( $p < 0.05$ ). These findings suggest combination therapy may provide a greater reduction in tumor growth than cisplatin monotherapy alone. Further comparison of EDC22 treatment to radiation therapy found there was a significant reduction in tumor growth following monotherapy with EDC22 relative to radiation therapy alone ( $p < 0.05$ ). However, there was no significant difference between the tumor growth in the EDC22 monotherapy and combination therapy cohorts. This is likely due to the significant reduction tumor growth with EDC22 monotherapy. In this study, the in vivo combination therapy experiments were designed with the hope of selecting treatment dosages for the monotherapy cohorts that would reduce tumor growth without resulting in complete shrinkage of the tumor. Ideally, this would allow for an improved response with the combination therapy. However, the potency of EDC22 observed in this study may be masking potential additive benefits of combination therapy. The results from this investigation suggest the potential for further reduction in the treatment dosage of EDC22 for future experiments.

This preliminary investigation demonstrated the potent antitumorigenic effects of EDC22. Further investigations are warranted to determine the effects of EDC22 treatment on the

cellular components of the tumor microenvironment (fibroblasts, endothelial cells, and angiogenesis), and the effects of EDC22 on receptor profiling of HNSCC, normal and supporting cells. There is potential for treatment toxicity associated with this agent given the large variety of cell types that express CD147. The extent of toxicity will likely be mild since normal cells express much lower levels of CD147 relative to dysplastic and squamous cell carcinoma cells [22,24,43–45,20]. Additionally, the anti-CD147 monoclonal antibody used in this investigation targeted human CD147, not murine CD147. Although human and murine CD147 are highly homologous, with 51% homology of the extracellular domain [46], this still limits the ability to draw conclusions on toxicity. A greater understanding of the effects of EDC22 on other cell lines and receptor profiling would help determine which combination therapies may be of added benefit, as well as which patient population would benefit the greatest from treatment with EDC22.

In this preliminary investigation we demonstrated EDC22 has significant potency and efficacy in the preclinical treatment of HNSCC. EDC22 was found to have a potent anti-carcinogenic effect on HNSCC cells in vitro and in vivo. By combining the strengths of two treatment modalities (potent, toxic small molecule inhibitor and a targeted, highly specific monoclonal antibody), EDC22 has the potential to significantly reduce HNSCC oncogenesis while minimizing side effects and maximizing therapeutic efficacy. Therefore, further investigations into its clinical efficacy and potential toxicity to normal tissues are warranted.

## Acknowledgments

This study was supported jointly by grants for the National Institute of Health (R01CA142637-01, 2T32CA091078-09, and 1G20RR022807-01). The funding source had no role in experimental design or manuscript composition. The authors would like to thank Tong Zhou, Ph.D. for producing and providing us with the anti-CD147 monoclonal antibody.

## Abbreviation

HNSCC      head and neck squamous cell carcinoma

## References

1. Mamelle G. Selective neck dissection and sentinel node biopsy in head and neck squamous cell carcinomas. *Recent Res Can Res.* 2000; 157:193–200.
2. Mamelle G, Pampurik J, Luboinski B, Lancar R, Lusinchi A, Bosq J. Lymph node prognostic factors in head and neck squamous cell carcinomas. *Am J Surg.* 1994; 168:494–8. [PubMed: 7977983]
3. Hauswald H, Simon C, Hecht S, Debus J, Lindel K. Long-term outcome and patterns of failure in patients with advanced head and neck cancer. *Radiat Oncol.* 2011; 6:70. [PubMed: 21663634]
4. Woolgar JA, Beirne JC, Vaughan ED, Lewis-Jones HG, Scott J, Brown JS. Correlation of histopathologic findings with clinical and radiologic assessments of cervical lymph-node metastases in oral cancer. *Int J Oral Maxillofac Surg.* 1995; 24:30–7. [PubMed: 7782638]
5. Woolgar JA, Rogers SN, Lowe D, Brown JS, Vaughan ED. Cervical lymph node metastasis in oral cancer: the importance of even microscopic extracapsular spread. *Oral Oncol.* 2003; 39:130–7. [PubMed: 12509965]
6. Tankere F, Camproux A, Barry B, Guedon C, Depondt J, Gehanno P. Prognostic value of lymph node involvement in oral cancers: a study of 137 cases. *Laryngoscope.* 2000; 110:2061–5. [PubMed: 11129021]
7. Kowalski LP, Bagietto R, Lara JR, Santos RL, Silva JF Jr, Magrin J. Prognostic significance of the distribution of neck node metastasis from oral carcinoma. *Head Neck.* 2000; 22:207–14. [PubMed: 10748442]



8. de Aguiar AF Jr, Kowalski LP. Clinicopathological and immunohistochemical evaluation of oral squamous cell carcinoma in patients with early local recurrence. *Oral Oncol.* 2007; 43:593–601. [PubMed: 17070093]
9. Okada Y. Relationships of cervical lymph node metastasis to histopathological malignancy grade, tumor angiogenesis, and lymphatic invasion in tongue cancer. *Odontology.* 2010; 98:153–9. [PubMed: 20652794]
10. Leong SC, Kartha SS, Kathan C, Sharp J, Mortimore S. Outcomes following total laryngectomy for squamous cell carcinoma: one centre experience. *Eur Ann Otorhinolaryngol Head Neck Dis.* 2012
11. MaJ, Liu Y.; Huang, XL., et al. Induction chemotherapy decreases the rate of distant metastasis in patients with head and neck squamous cell carcinoma but does not improve survival or locoregional control: a meta-analysis. *Oral Oncol.* 2012
12. Kanotra SP, Kanotra S, Gupta A, Paul J. Chemoradiation in advanced head and neck cancers: a comparison of two radiosensitizers, paclitaxel and cisplatin. *Indian J Otolaryngol Head Neck Surg.* 2011; 63:229–36. [PubMed: 22754800]
13. Krstevska V, Stojkovski I, Zafirova-Ivanovska B. Concurrent radiochemotherapy in locally-regionally advanced oropharyngeal squamous cell carcinoma: analysis of treatment results and prognostic factors. *Radiat Oncol.* 2012; 7:78. [PubMed: 22640662]
14. Chen H, Zhou L, Chen D, Luo J. Clinical efficacy of neoadjuvant chemotherapy with platinum-based regimen for patients with locoregionally advanced head and neck squamous cell carcinoma: an evidence-based meta-analysis. *Ann Saudi Med.* 2011; 31:502–12. [PubMed: 21911989]
15. Zhang S, Chen J, Jiang H, Ma H, Yang B. Anti-epidermal growth factor receptor therapy for advanced head and neck squamous cell carcinoma: a meta-analysis. *Eur J Clin Pharmacol.* 2012; 68:561–9. [PubMed: 22231637]
16. Teicher BA, Chari RV. Antibody conjugate therapeutics: challenges and potential. *Clin Cancer Res.* 2011; 17:6389–97. [PubMed: 22003066]
17. Geering K. Functional roles of Na,K-ATPase subunits. *Curr Opin Nephrol Hypertens.* 2008; 17:526–32. [PubMed: 18695395]
18. Lingrel J, Moseley A, Dostanic I. Functional roles of the alpha isoforms of the Na,K-ATPase. *Ann NY Acad Sci.* 2003; 986:354–9. [PubMed: 12763850]
19. Cheng MF, Tzao C, Tsai WC. Expression of EMMPRIN and matriptase in esophageal squamous cell carcinoma: correlation with clinicopathological parameters. *Dis Esophagus.* 2006; 19:482–6. [PubMed: 17069593]
20. Huang Z, Huang H, Li H, Chen W, Pan C. EMMPRIN expression in tongue squamous cell carcinoma. *J Oral Pathol Med.* 2009; 38:518–23. [PubMed: 19473445]
21. Ishibashi Y, Matsumoto T, Niwa M, et al. CD147 and matrix metalloproteinase-2 protein expression as significant prognostic factors in esophageal squamous cell carcinoma. *Cancer.* 2004; 101:1994–2000. [PubMed: 15372476]
22. Rosenthal EL, Shreenivas S, Peters GE, Grizzle WE, Desmond R, Gladson CL. Expression of extracellular matrix metalloprotease inducer in laryngeal squamous cell carcinoma. *Laryngoscope.* 2003; 113:1406–10. [PubMed: 12897567]
23. Lescaille G, Menashi S, Cavelier-Balloy B. EMMPRIN/CD147 up-regulates urokinase-type plasminogen activator: implications in oral tumor progression. *BMC Cancer.* 2012; 12:115. [PubMed: 22443116]
24. Vigneswaran N, Beckers S, Waigel S, et al. Increased EMMPRIN (CD 147) expression during oral carcinogenesis. *Exp Mol Pathol.* 2006; 80:147–59. [PubMed: 16310185]
25. Marieb EA, Zoltan-Jones A, Li R. Emmprin promotes anchorage-independent growth in human mammary carcinoma cells by stimulating hyaluronan production. *Cancer Res.* 2004; 64:1229–32. [PubMed: 14983875]
26. Newman JR, Bohannon IA, Zhang W, Skipper JB, Grizzle WE, Rosenthal EL. Modulation of tumor cell growth in vivo by extracellular matrix metalloprotease inducer. *Arch Otolaryngol Head Neck Surg.* 2008; 134:1218–24. [PubMed: 19015455]

27. Wang CH, Yao H, Chen LN, et al. CD147 induces angiogenesis through vascular endothelial growth factor and hypoxia-inducible transcription factor 1 $\alpha$ -mediated pathway in rheumatoid arthritis. *Arthritis Rheum.* 2011
28. Yan L, Zucker S, Toole BP. Roles of the multifunctional glycoprotein, emmprin (basigin; CD147), in tumour progression. *Thromb Haemost.* 2005; 93:199–204. [PubMed: 15711733]
29. Yang JM, Xu Z, Wu H, Zhu H, Wu X, Hait WN. Overexpression of extracellular matrix metalloproteinase inducer in multidrug resistant cancer cells. *Mol Cancer Res.* 2003; 1:420–7. [PubMed: 12692261]
30. Heller M, von der Ohe M, Kleene R, Mohajeri MH, Schachner M. The immunoglobulin-superfamily molecule basigin is a binding protein for oligomannosidic carbohydrates: an anti-idiotypic approach. *J Neurochem.* 2003; 84:557–65. [PubMed: 12558975]
31. Langenhan JM, Peters NR, Guzei IA, Hoffmann FM, Thorson JS. Enhancing the anticancer properties of cardiac glycosides by neoglycorandomization. *Proc Natl Acad Sci USA.* 2005; 102:12305–10. [PubMed: 16105948]
32. Harris LJ, Skaletsky E, McPherson A. Crystallographic structure of an intact IgG1 monoclonal antibody. *J Mol Biol.* 1998; 275:861–72. [PubMed: 9480774]
33. Ogawa H, Shinoda T, Cornelius F, Toyoshima C. Crystal structure of the sodium-potassium pump (Na<sup>+</sup>, K<sup>+</sup>-ATPase) with bound potassium and ouabain. *Proc Natl Acad Sci USA.* 2009; 106:13742–7. [PubMed: 19666591]
34. Hamblett KJ, Senter PD, Chace DF. Effects of drug loading on the antitumor activity of a monoclonal antibody drug conjugate. *Clin Cancer Res.* 2004; 10:7063–70. [PubMed: 15501986]
35. Jeffrey SC, Andreyka JB, Bernhardt SX. Development and properties of beta-glucuronide linkers for monoclonal antibody–drug conjugates. *Bioconjug Chem.* 2006; 17:831–40. [PubMed: 16704224]
36. Polson AG, Calemine-Fenaux J, Chan P, et al. Antibody–drug conjugates for the treatment of non-Hodgkin's lymphoma: target and linker-drug selection. *Cancer Res.* 2009; 69:2358–64. [PubMed: 19258515]
37. Sanderson RJ, Hering MA, James SF, et al. In vivo drug-linker stability of an anti-CD30 dipeptide-linked auristatin immunoconjugate. *Clin Cancer Res.* 2005; 11:843–52. [PubMed: 15701875]
38. Seftor RE, Seftor EA, Grimes WJ, et al. Human melanoma cell invasion is inhibited in vitro by swainsonine and deoxymannojirimycin with a concomitant decrease in collagenase IV expression. *Melanoma Res.* 1991; 1:43–54. [PubMed: 1668368]
39. Sun MM, Beam KS, Cervený CG, et al. Reduction-alkylation strategies for the modification of specific monoclonal antibody disulfides. *Bioconjug Chem.* 2005; 16:1282–90. [PubMed: 16173809]
40. Dean NR, Helman EE, et al. Anti-EMMPRIN monoclonal antibody as a novel agent for therapy of head and neck cancer. *Clin Cancer Res.* 2009; 15:4058–65. [PubMed: 19509148]
41. Sano D, Matsumoto F, Valdecanas DR, et al. Vandetanib restores head and neck squamous cell carcinoma cells' sensitivity to cisplatin and radiation in vivo and in vitro. *Clin Cancer Res.* 2011; 17:1815–27. [PubMed: 21350000]
42. Ekshyyan O, Rong Y, Rong X, et al. Comparison of radiosensitizing effects of the mammalian target of rapamycin inhibitor CCI-779 to cisplatin in experimental models of head and neck squamous cell carcinoma. *Mol Cancer Ther.* 2009; 8:2255–65. [PubMed: 19625495]
43. DeCastro R, Zhang Y, Guo H, et al. Human keratinocytes express EMMPRIN, an extracellular matrix metalloproteinase inducer. *J Invest Dermatol.* 1996; 106:1260–5. [PubMed: 8752667]
44. Sameshima T, Nabeshima K, Toole BP, et al. Expression of emmprin (CD147), a cell surface inducer of matrix metalloproteinases, in normal human brain and gliomas. *Int J Cancer.* 2000; 88:21–7. [PubMed: 10962435]
45. Bordador LC, Li X, Toole B. Expression of emmprin by oral squamous cell carcinoma. *Int J Cancer.* 2000; 85:347–52. [PubMed: 10652425]
46. Miyauchi T, Masuzawa Y, Muramatsu T. The basigin group of the immunoglobulin superfamily: complete conservation of a segment in and around transmembrane domains of human and mouse basigin and chicken HT7 antigen. *J Biochem.* 1991; 110:770–4. [PubMed: 1783610]

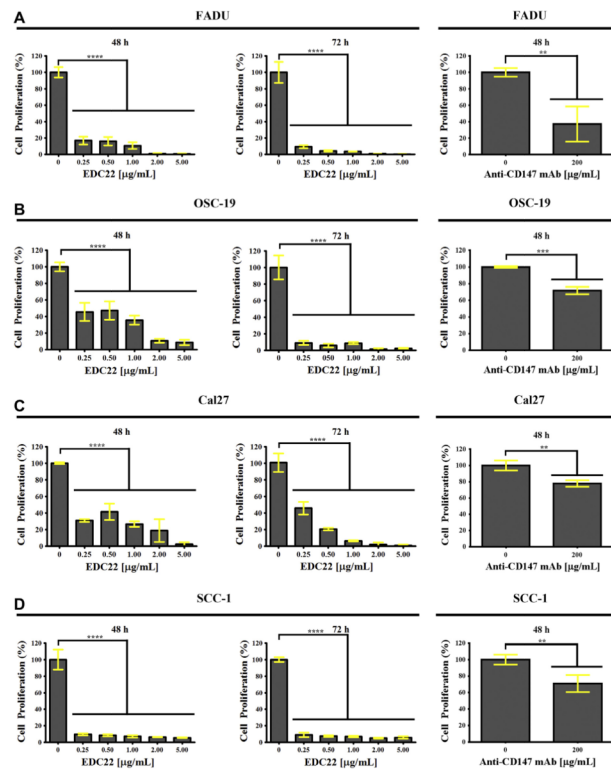


**Figure 1.**

In vitro proliferation of HNSCC cells FADU (A), OSC-19 (B), Cal27 (C) and SCC-1 (D) was significantly reduced following treatment with EDC22 (0–5.0  $\mu\text{g/mL}$ ) for 48 h and 72 h and with anti-CD147 mAb (200  $\mu\text{g/mL}$ ) for 48 h. Statistical significance by unpaired *t*-test, \*\*  $p < 0.01$ , \*\*\*  $p < 0.001$ , and \*\*\*\*  $p < 0.0001$ . Columns, mean for triplicate and bars, SD.

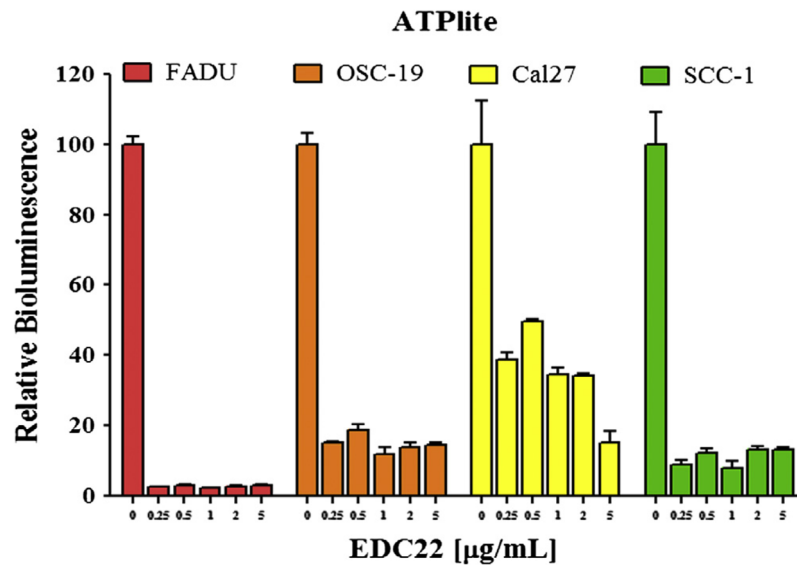


**Figure 2.**

In vitro treatment of HNSCC cells (FADU, OSC-19, Cal27, SCC-1) with EDC22 (0–5.0 µg/mL) for 48 h resulted in a significant reduction in cell viability (ATPlite assay). Statistical significance by unpaired *t*-test, \*\*\*\* $p < 0.0001$ . Columns, mean for triplicate and bars, SD.

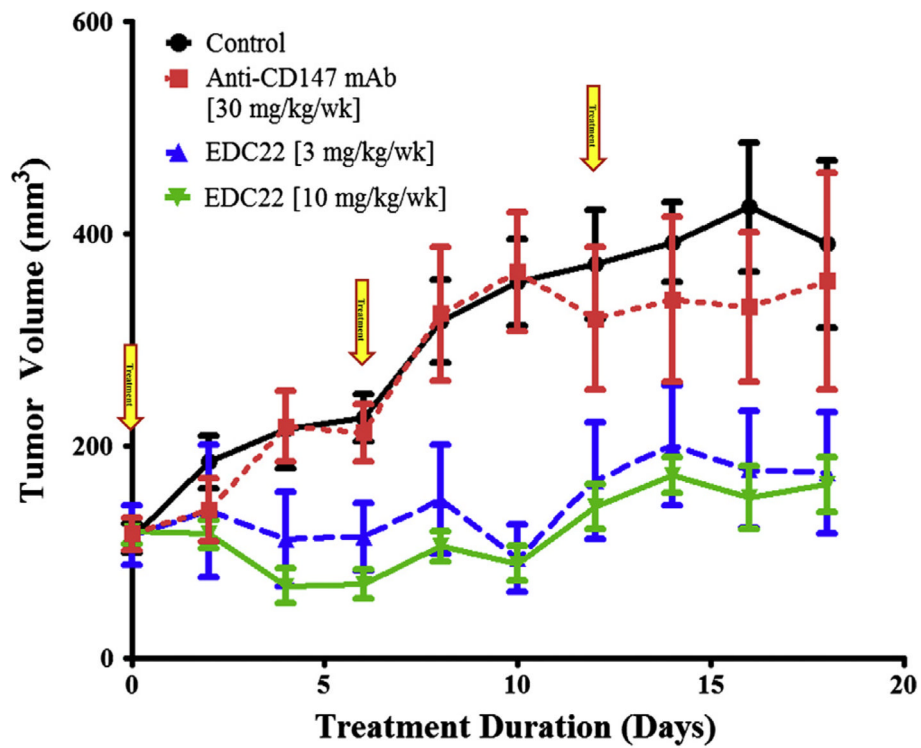


**Figure 3.** Assessment of EDC22 on in vivo tumor growth in an oral cavity orthotopic tongue model. OSC-19 cells lines were implanted in the proximal tongue of athymic nude mice ( $n = 5/\text{group}$ ). Relative to control and anti-CD147 treatment cohorts, both EDC22 treatment cohorts demonstrated significantly smaller tumor volumes on day 8 and day 10 relative to controls ( $p < 0.01$ ). Marker, mean; bars, SD; and arrow, timing of treatment.



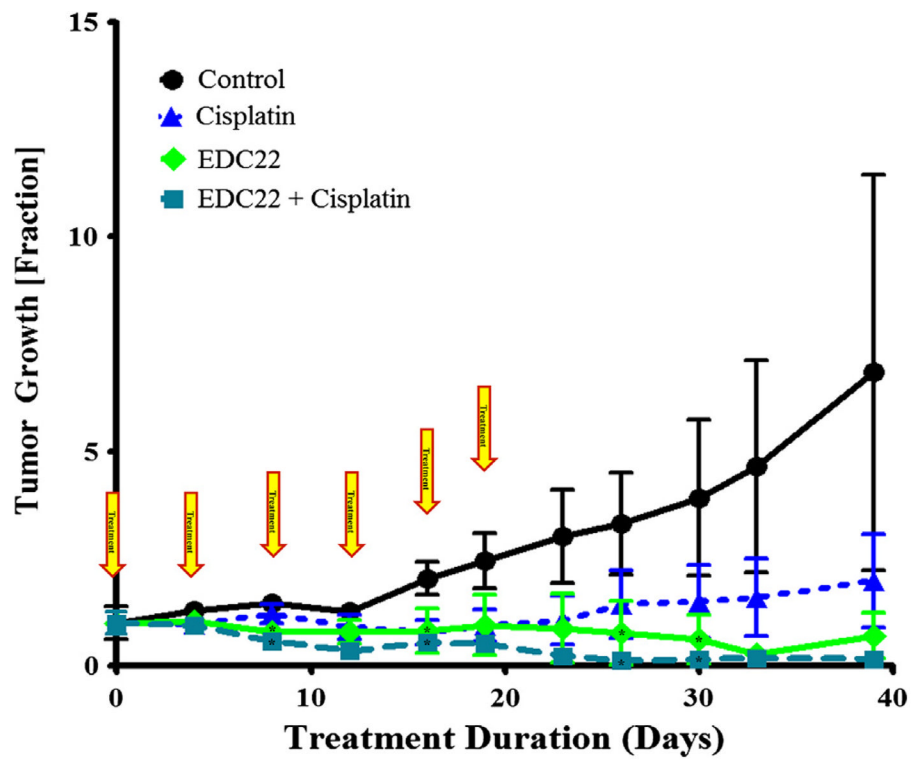


**Figure 4.** Assessment of EDC22 and cisplatin therapy on in vivo tumor growth in murine flank model (SCC-1). In vivo comparison of tumor growth following treatment with EDC22 (3 mg/kg twice wk) compared to cisplatin (1 mg/kg/wk). Statistical significance by unpaired *t*-test (treatment relative to control), \**p* < 0.05. Marker, mean; bars, SD; and arrow, timing of treatment.

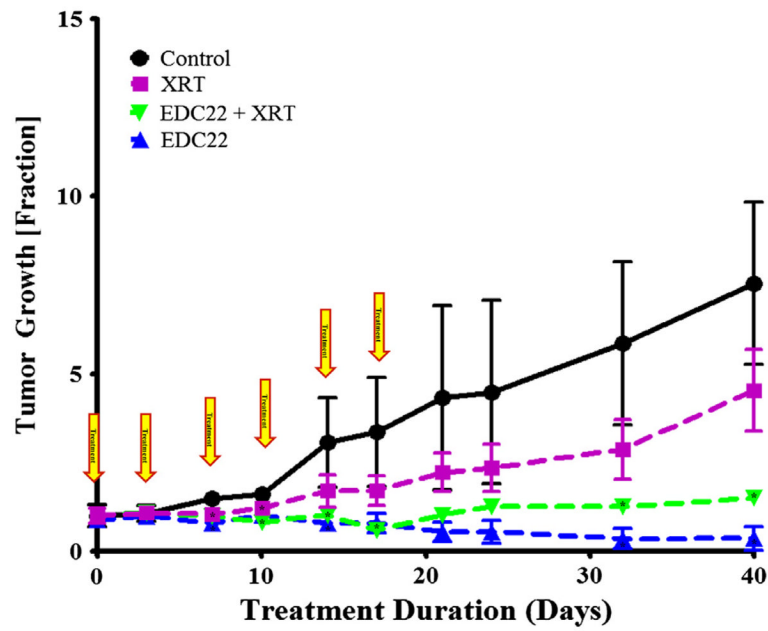


**Figure 5.**

Assessment of EDC22 and radiation therapy on in vivo tumor growth in murine flank model (SCC-1). SCC-1 flank xenografts were divided into four cohorts: control, radiation therapy (XRT) monotherapy, EDC22 (3 mg/kg twice wk) monotherapy and combination treatment. Statistical significance by unpaired *t*-test (treatment relative to control), \**p* < 0.05. Marker, mean; bars, SD; and arrow, timing of EDC22 treatment.